Transdiagnostic characterization of neuropsychiatric disorders by hyperexcitation-induced immaturity (100 characters)

Tomoyuki Murano[1,2,3], Hideo Hagihara[1], Katsunori Tajinda[4], Mitsuyuki Matsumoto[5], Tsuyoshi Miyakawa[1]*

[1]Division of Systems Medical Science, Institute for Comprehensive Medical Science, Fujita Health University, Japan

[2]Department of Physiological Science, School of Life Science, The Graduate University for Advanced Studies, Japan [SOKENDAI]

[3]Division of Cell Signaling, National Institute for Physiological Sciences, Japan

[4] Neuroscience, La Jolla Laboratory, Astellas Research Institute of America LLC, USA

[5] Drug Discovery Research, Astellas Pharma Inc., Japan

*Correspondence: miyakawa@fujita-hu.ac.jp

Abstract

Biomarkers are needed to improve the diagnosis of neuropsychiatric disorders. Promising candidates are imbalance of excitation and inhibition in the brain, and maturation abnormalities. Here, we characterized different disease conditions by mapping changes in the expression patterns of maturation-related genes whose expression was altered by experimental neural hyperexcitation in published studies. This revealed two gene expression patterns: decreases in maturity markers and increases in immaturity markers. These two groups of genes were characterized by the overrepresentation of genes related to synaptic function and chromosomal modification, respectively. We used these two groups in a transdiagnostic analysis of 80 disease datasets for eight neuropsychiatric disorders and 12 datasets from corresponding animal models, and found that transcriptomic pseudoimmaturity inducible by neural hyperexcitation is shared by multiple neuropsychiatric disorders, such as schizophrenia, Alzheimer disorders, and ALS. Our results indicate that this endophenotype serve as a basis for transdiagnostic characterization of these disorders.

(147 words)

Introduction

Neuropsychiatric disorders—such as schizophrenia, bipolar disorder, major depression disorders, and autism spectrum disorder—are common, with over a third of the population in most countries being diagnosed with at least one such disorder at some point in their life[1]. Almost all neuropsychiatric disorders are currently classified mainly on the basis of clinical signs and symptoms. However, there is evidence that patients with different clinical diagnoses share similar biological features, such as genetic mutations, molecular expression, or brain activity[2–6]. Recently, psychiatry has undergone a tectonic shift to incorporate the concepts of modern biology. There have been recent attempts to reclassify psychiatric disorders according to biological domains (e.g. genes, neural circuits, behavior), such as through the Research Domain Criteria (RDoC) initiative[7]. Therefore, identifying appropriate biomarkers which can be used for transdiagnostic assessment of neuropsychiatric disorders is essential for better classification of these diseases and understanding of their biological basis.

Using coexpression network analysis, a recent study revealed that cross-disorder gene expression overlaps could be used to characterize five major neuropsychiatric disorders[8]. Some of these overlapping gene groups were biologically well-characterized by Gene Ontology enrichment or cell-type specificity, but the biological properties of other gene groups were rather unclear. Thus, non-biased coexpression network analyses do not necessarily detect modules that extract the biological features of neuropsychiatric disorders. Then, to achieve better characterization of neuropsychiatric disorders, it might be helpful to detect modules of coexpressed genes and conduct gene expression analysis based on the findings derived from researches on animal models of neuropsychiatric disorders.

To date, we have screened more than 180 strains of genetically engineered mice using a large-scale and comprehensive battery of behavioral tests, and identified several strains with abnormal behaviors related to neuropsychiatric disorders such as schizophrenia, bipolar disorder, and intellectual disability[9]. We discovered common endophenotypes in the brains of multiple strains of these genetically engineered mice with behavioral abnormalities. We termed one such endophenotype in the hippocampus of adult mice the “immature dentate gyrus (iDG)” phenotype[10–13]. In this phenotype, the molecular and electrophysiological properties of adult DG neurons in the genetically engineered mice were similar to those of immature DG neurons in typically developing infants. For example, the expression of calbindin, a marker of maturity in DG neurons, was decreased and the expression of calretinin, a marker of immaturity, was increased[10–15]. Similar molecular changes to some of those found in mice with iDG have been observed in the postmortem brains of patients with schizophrenia[16], bipolar disorder[16], and epilepsy[17–19]. Furthermore, there is growing evidence that changes in molecular markers of

pseudoimmaturity are also observed in other brain areas of patients with schizophrenia[20-28], bipolar disorder[26], autism[26], and alcoholism[29]. Therefore, we proposed that pseudoimmaturity of the brain could potentially be a useful transdiagnostic biomarker[9].

Pseudoimmaturity of the brain can be induced in adulthood. Previously, we found that chronic fluoxetine treatment reverses the maturation status of DG neurons in adult wild-type mice, a phenomenon that we termed "dematuration"[30,31]. Likewise, recent studies suggest that several maturation-related genes and electrophysiological properties in the DG of wild-type adult mice assume an immature-like status after treatment with pilocarpine or electroconvulsive stimulation[16,32]. As mentioned above, an iDG-like phenotype has been found in patients with epilepsy[17–19]. Therefore, we hypothesized that the hyperexcitation of neurons may be a cause of pseudoimmaturity of the brain in adulthood.

Some studies suggest that hyperexcitation of neurons may underlie abnormalities related to certain types of neuropsychiatric disorders. Individuals with epilepsy are at increased risk of developing schizophrenia, and vice versa[33,34] , and patients with epilepsy can also display psychotic symptoms that resemble those found in patients with schizophrenia[35]. Imbalances in excitatory and inhibitory brain circuitry have been proposed to be involved in the pathogenesis and pathophysiology of schizophrenia[36–39]. Hyperactive action-potential firing has also been observed in hippocampal granule-cell-like neurons derived from induced pluripotent stem cells (iPSCs) of patients with bipolar disorder[40]. Recent studies suggested that human patients with Alzheimer's disease and temporal lobe epilepsy may harbor common underlying mechanisms[17,41–43]. Considering these findings, we hypothesized that the immature-like gene expression patterns induced by neural hyperexcitation may overlap with the abnormal gene expression patterns in the brains of patients with neuropsychiatric disorders and the related animal models. If this is the case, we hypothesized that this overlap can be used to perform transdiagnostic characterization of neuropsychiatric disorders.

To test this hypothesis, we first performed a meta-analysis of microarray datasets, comparing the changes in gene expression in rat DG after seizure induction with the differences in gene expression in infant mice versus adult mice. To assess consistency across species, we also conducted a similar comparison with human fetal hippocampus. The overlap between gene sets was estimated using the Running Fisher test[44], which is a nonparametric rank-based statistical method developed by BSCE. This method enables us to statistically assess the pairwise correlations between any two datasets, including datasets from different species and organs[28,29,45,46]. The gene expression patterns in rat DG after seizure induction significantly overlapped with those specific to immature mouse DG and also with those specific to early-stage human fetal hippocampus. From the set of overlapping genes, we

105 defined two groups; maturity-marker genes and immaturity-marker genes that are inducible by
106 neural hyperexcitation. We assessed the expression patterns of these two groups of
107 maturation-related genes in 80 public gene-expression datasets derived from the postmortem
108 brains of patients with various neuropsychiatric disorders and from neural cells derived from
109 patient iPSCs, and in a further 12 datasets from the brains of related animal models. Through
110 this analysis, we characterized the expression patterns of maturation-related genes that are
111 inducible by neural hyperexcitation across different disease conditions.
112 (932 words)
113

Results

Neural hyperexcitation induces immature-like gene expression patterns in DG

To examine the developmental changes in gene expression patterns in the rodent DG, we created a microarray dataset from postnatal day 8, 11, 14, 17, 21, 25, and 29 infant mice (GSE113727) and compared it with a dataset from 33-week-old adult mice (GSE42778)[12]. Within the entire mice DG dataset, the largest overlap for changes in gene expression after pilocarpine injection was for the comparison between day 8 infant and 33-week-old adult mice (Figure S1a). We included the dataset from postnatal day 8 infant mice for subsequent analysis. The expression levels of 6552 genes were increased in the DG of infant mice compared with adult mice, whereas the expression levels of 8637 genes were decreased (absolute fold change > 1.2 and t-test $P < 0.05$). Next, we assessed the changes in gene expression induced by neural hyperexcitation in a rodent model. We obtained publicly available microarray datasets from the DG of adult rats after seizures induced by injection of pilocarpine (GSE47752)[47]. The expression levels of 7073 genes were significantly changed in the DG of epileptic-seizure rats 1 day after pilocarpine injection compared with rats treated with saline (absolute fold change > 1.2, $P < 0.05$).

To investigate whether the neuronal hyperexcitation datasets contain immature-like gene expression patterns, we assessed the overlap between the set of genes with altered expression in immature mice and the set of genes with altered expression in adult seizure-model rats, using the Running Fisher algorithm on the BaseSpace platform to determine the significance of the overlap (see Supplementary Methods for Details). We found a striking degree of similarity: 2807 genes showed changes in expression in both datasets (overlap $P = 3.8 \times 10^{-11}$) (Figure 1a). Among these 2807 genes, we named the 726 genes whose expression levels decreased in both datasets “hyperexcitation-induced maturity-related genes” (hiM genes (mouse): green bar in Figure 1a) and the 938 genes whose expression levels increased in both datasets “hyperexcitation-induced immaturity-related genes” (hiI genes (mouse): red bar in Figure 1a). The comprehensive gene lists of hiM and hiI genes are in Table S1 (Table S1: hiM/hiI_GeneList). The overlap for genes with positively correlated expression (red and green bars) was larger than the overlap for genes with negatively correlated expression (light and dark yellow bars), indicating that the direction of expressional changes in the two datasets are more alike than they are different. These results suggest that neuronal hyperexcitation induces a pattern of immature-like gene expression in the adult DG.

Next, we compared the changes in expression during development in the human fetal hippocampus with those in rats after seizure induction to assess consistency across species. We

obtained publicly available microarray datasets for the human fetal hippocampus during development (GSE25219)[48]. Within the entire fetal hippocampal dataset, the largest overlap for changes in gene expression after pilocarpine injection was for the comparison between 8–9-week fetuses and 19–23-week fetuses (Figure S1b). We again found a striking degree of similarity: 2043 genes showed changes in expression in both datasets (overlap $P = 1.8 \times 10^{-12}$) (Figure 1b). Among these 2043 genes, we termed the 579 genes whose expression decreased in both datasets "hiM genes (human)" (green bar in Figure 1b) and the 716 genes whose expression increased in both datasets "hiI genes (human)" (red bar in Figure 1b). The overlap for genes with positively correlated expression (red and green bars) were larger than those with negatively correlated expression (light and dark yellow bars), suggesting that, similar to the results in mice, the gene expression changes in rat DG after seizure induction are comparable to the reverse of the changes that occur as the human hippocampus develops.

Hyperexcitation-induced maturity- and immaturity-related genes exhibit different biological properties

To characterize the biological features associated with the hiM and hiI gene groups in mouse and human, we conducted pathway enrichment analyses in BaseSpace. The 20 biogroups with the most significant overlap with hiM and hiI genes are listed in Table 1a and 1b. Among mouse hiM genes, 4 out of the top 20 biogroups are associated with synapse and channel activity (e.g., transmission of nerve impulse, synapse, and synaptic transmission) (Table 1a), whereas among human hiM genes, 6 out of the top 20 biogroups are also associated with synapse and channel activity (e.g., transmission of nerve impulse, synaptic transmission, axon, and synapse) (Table 1b).

Among the mouse hiI genes, 4 out of the top 20 biogroups were associated with the nucleus (e.g., genes involved in the cell cycle and genes involved in DNA replication) (Table 1a). Among the human hiI genes, 15 out of the top 20 biogroups were associated with the nucleus (e.g., genes involved in the cell cycle, chromosomes, and response to DNA damage stimulus) (Table 1b). It is noteworthy that there is little overlap in the top 20 biogroups for the hiM and hiI genes (Table 1a, 1b). Thus, the biogroups related to the hiM and hiI genes are likely to be functionally different.

We also compared datasets from the DG of typically developing infants with datasets from rat DG at three different timepoints after seizure induction by injection of pilocarpine or kainite (day 1, day 3, and day 10) ,and performed principal component analysis on the changes in mouse hiM/hiI genes at different timepoints (Figure S2a, S2b; Supplementary Results). The time-course of changes in the mouse hiM genes after seizure induction was different from the

time-course of changes in the mouse hiI genes. In addition, we conducted a spatial pattern analysis of the mouse hiM/hiI genes, which indicated that their protein products have slightly different patterns of subcellular localization (Figure S2c; Supplementary Results). The mouse hiM genes tend to be strongly expressed at the plasma membrane, with expression changes stabilizing by the third day after seizure induction. By contrast, the hiI genes tend to be expressed in the nucleus and changes in expression after seizure induction are slower to stabilize. Together, these results indicate that the hiM/hiI genes have different spatiotemporal patterns of changes in expression.

Gene expression patterns in patients can be characterized in terms of hiM/hiI genes

Next, we investigated whether and to what extent the expression changes in maturation-related genes induced by hyperexcitation overlap with gene expression patterns in various neuropsychiatric disorders. As above, we evaluated similarities between the changes in gene expression patterns in different groups using overlap *P*-values calculated by Running Fisher algorithm (Figure 2a). Similarity indexes for each comparison were defined as the −log of the overlap *P*-values with hiM or hiI genes, denoted by hiM-index or hiI-index, respectively. High values in hiM-/hiI-index represent that there is large overlap between the dataset analyzed and hiM/hiI genes. We obtained the hiM-/hiI-indexes for the datasets from human patients and plotted them in two-dimensional (2-D) space to show the extent of overlap between datasets and hiM/hiI genes (Figure 2a).

We initially performed this 2-D analysis on a dataset containing the expression profile of the prefrontal cortex in the postmortem brains of patients with schizophrenia (schizophrenia dataset #1: details in Table S2) (Figure 2b). The expression of 1744 genes differed between patients and healthy controls (significance level of 0.05). The numbers of hiM and hiI genes with altered expression in schizophrenia dataset #1 were 87 and 76, respectively, and the overlap *P*-values were 2.4×10^{-10} and 6.9×10^{-7}. The hiM-index and hiI-index for this dataset were 9.62 ($= -\log(2.4\times10^{-10})$) and 6.16 ($= -\log(6.9\times10^{-7})$). This result corresponds to a point in 2-D space (Figure 2b). Points that fall below the unity line (dashed line) indicate datasets in which changes in hiM genes are dominant, whereas points above the unity line indicate datasets with dominant changes in hiI genes. The angle from unity line indicates the degree of the hiM-/hiI- dominance. The same analysis was performed for other schizophrenia datasets (schizophrenia datasets #2–#16), including ones obtained from different areas of the postmortem brain and from cultured neurons derived from the iPSCs of patients. Scatter plots of the results from the schizophrenia datasets are shown in Figure 3a. Thirteen out of sixteen points were below the unity line. Most of the schizophrenia datasets exhibited hiM-index

dominant patterns, showing high hiM-index values and low hiI-index values (Figure 3a).

We extended the same analysis to 80 disease datasets from seven other neuropsychiatric diseases (amyotrophic lateral sclerosis (ALS), Alzheimer's disease (AD), autism spectrum disorder (ASD), Parkinson's disease (PD), bipolar disorder (BPD), Huntington's disease (HD), and major depressive disorder (MDD); Table S2). Results of each dataset are shown in Figure 3b-3h. Overall distribution patterns of each disease are shown in Figure 3i. The ALS datasets tended to show higher hiI-index values than hiM-index values, indicating hiI-index-dominant pattern (Figure 3b). The AD datasets showed different patterns in the hiM-/hiI-index depending on the type of sample; datasets from the postmortem brains of patients with AD tended to show high values only in the hiM-index, and datasets from patient iPSCs tended to show high values only in the hiI-index (Figure 3c). Datasets from ASD did not show any dominant patterns either in the hiM-index or hiI-index (Figure 3d). Most datasets from patients with PD, BPD, HD, and MDD did not show pronounced values in the hiM-index or the hiI-index (Figure 3e, 3f, 3g, 3h).

Thus, the 2-D analysis revealed that some neuropsychiatric diseases have characteristic patterns in the hiM-/hiI-indexes: for example, most datasets from patients with schizophrenia exhibited a higher hiM-index than hiI-index, whereas ALS datasets showed hiI-index-dominant pattern (Figure 3i). Meanwhile, different diseases sometimes show similar changes in the hiM- or hiI-index; for example, some of the schizophrenia, ASD, and AD datasets shared a high hiM-index, and some of the ALS, and AD datasets shared a high hiI-index. The other four diseases—PD, BPD, HD, and MDD—did not show pronounced changes in hiM-/hiI-indexes, suggesting that these diseases may not share endophenotype as pseudoimmaturity inducible by neural hyperexcitation. These results raise the possibility that there are patterns of gene-expression perturbations that are shared and distinct across these neuropsychiatric disorders.

Genetic and environmental risk factors induce changes in the pattern of expression of hiM/hiI genes

Previous studies suggest that many genetic risk and environmental factors, such as seizure, hypoxia, and infection, contribute to the development of neuropsychiatric disorders[2,49,50]. We next applied the 2-D analysis technique to datasets from genetic animal models of disorders and from animals that experienced risk events.

First, we obtained publicly available datasets for mice that had experienced putative risk events for schizophrenia, bipolar disorders, and Alzheimer's disease, including seizure (#1: GSE49030, #2: GSE4236)[51,52], ischemia (#1: GSE32529, #2: GSE35338)[1–3], and infection

(mimicked by CpG; GSE32529)[53,54]. All the studies used here included datasets for different time points after the risk event; hence, we were able to examine the time-course of changes in the hiM- and hiI-indexes to reveal the short- and long-term effect of risk event on expression patterns of hiM/hiI genes. The results showed that datasets from mouse hippocampus treated with kainite, seizure-inducing drug, exhibited time-course changes in the hiM- and hiI-indexes: the hiM-index tended to be dominant in the early stage after seizure induction, and the hiI-index became more dominant in the late stages (Figure 4a: seizure #1). The results from other datasets on seizure, ischemia, and infection showed roughly similar time-course pattern changes in the hiM- and hiI-indexes as those observed in seizure dataset #1, being relatively hiM-index-dominant in the early stage, and then relatively hiI-index-dominant in the later stage (Figure 4a: seizure, ischemia, and CpG infection). These results indicate that different types of putative risk events for neuropsychiatric disorders induce roughly similar time-course changes in the expression of maturation-related genes induced by neural hyperexcitation.

Next, we obtained datasets from animal models with a genetic risk of a neurodegenerative disease: mice with transgenic expression of a G93A mutant form of human SOD1, as a model of ALS (#1: GSE46298, #2: GSE18597)[55,56]; transgenic mice with mutant human amyloid precursor protein (APP) and presenilin1 (PSEN1) genes, which cause familial Alzheimer's disease (#1: GSE64398, #2: GSE64398)[57]; and Df16(A) heterozygous mice carrying a chromosome 16 deletion syntenic to human 22q11.2 microdeletions, as a model of schizophrenia (GSE29767)[58]. We also obtained datasets from Schnurri-2 (Shn-2) knockout mice as a model of schizophrenia[12] and intellectual disability[14,59,60] and from mice with heterozygous knockout of the alpha-isoform of calcium/calmodulin-dependent protein kinase II (alpha-CaMKII+/−)[10,13] as a model of bipolar disorder. We performed 2-D analysis on these datasets and evaluated the changes in the hiM-/hiI-indexes of these model mice. Both datasets from transgenic mice with a SOD1(G93A) mutation exhibited a higher hiI-index than hiM-index in the later stages of disease progression (Figure 4b). These hiI-index-dominant patterns were also observed in the results derived from human patients with ALS (Figure 3b). In the mice with mutant human APP and PSEN1, both the hiM- and hiI-indexes increased in dataset from hippocampus and only hiI-index increased in dataset from cortex during the course of disease progression (Figure 4c). These patterns are neutral or hiI-index-dominant. These patterns partially mimic the results from human patients with Alzheimer's disease (Figure 3c). The Df16(A) heterozygous mice and alpha-CaMKII+/− mice showed hiM-index-dominant patterns, which are similar to results from human patients with schizophrenia (Figure 4d). Shn-2 KO mice showed high values for both the hiM- and hiI-indexes (Figure 4d). Thus, the results from the 2-D analysis of animal models are to some

289 extent consistent with the results from human patients, indicating that these model mice share
290 similar patterns of pseudoimmaturity induced by neural hyperexcitation with those of human
291 patients.
292 (2236 words)
293

Discussion

In this study, we demonstrated that neural hyperexcitation induces changes in the pattern of gene expression in the DG that are significantly similar to the immature hippocampus of typically developing human fetuses. From the pool of genes, we identified two groups of genes, and found that these are shared by multiple neuropsychiatric disorders, such as schizophrenia, Alzheimer disorders, and ALS.

Many of the datasets from patients with schizophrenia and from the postmortem brains of patients with Alzheimer's disease exhibited hiM-index-dominant pattern changes. The hiM genes include a GABA receptor, voltage-dependent calcium channel, glutamate receptor, and voltage-dependent sodium channel (Table S1). These genes have been reported to be implicated in the pathological changes in the brains of patients with schizophrenia and Alzheimer's disease[61–64]. Thus, many of the synaptic genes that changed in the brains of patients with schizophrenia or Alzheimer's disease could be genes whose expression increases during maturation and decreases with neural hyperexcitation. Although reductions in the expression of some synaptic genes in these disorders are well documented, our results are the first to raise the possibility that neuronal hyperexcitation may also induce reductions in such synaptic molecules.

Most of the datasets from patients with ALS and Alzheimer's disease exhibited hiI-index-dominant patterns. The hiI genes include DNA methyltransferase, cyclin, cyclin-dependent kinase, integrin beta 3 binding protein, and tumor protein p53 (Table S1). These genes are known to be important in chromosomal modification and DNA repair, and abnormal functions of these systems have been observed in patients with ALS and Alzheimer's disease[65–69]. Thus, some of the genes that are considered to be important in the development of these disorders are immaturity-related genes, whose expressions decrease during maturation and can be increased by neural hyperexcitation.

As for the datasets from patients with PD, BPD, HD, and MDD, most of them did not show significant overlap either hiM or hiI genes, indicating that there might not be pathological changes of pseudoimmaturity inducible by neural hyperexcitation in the datasets of these four diseases. Thus, we suggest that gene expression analysis based on the findings derived from shared endophenotypes are helpful to conduct transdiagnostic characterization of neuropsychiatric disorders.

Our study has some limitations. First, the number of available datasets was limited. All the datasets except the one for mouse development were obtained from the BaseSpace Correlation Engine. On this platform, vast numbers (over 21,000) of complex biological and clinical datasets are available. Even though we used all the gene expression dataset hits from

our keyword query to avoid sampling bias, the number of datasets was still small, from 8 datasets for ALS to 16 datasets for schizophrenia. Further accumulation of the studies will improve the reliability of our results. Another limitation is that the datasets used in this study are from different types of sample, including various central nervous system areas, such as the hippocampus, prefrontal cortex, striatum, and the spinal cord. The gene expression abnormalities in patients could differ depending on the brain area[48]. We also used datasets from cultured neurons differentiated from the iPSCs of human subjects, and it is controversial whether the pattern of gene expression in these neurons is comparable with that of neurons in the patients' brains[70,71]. It is also possible that the altered gene expression in the postmortem brains is due to the effects of medication rather than pathological changes from the disease itself[72]. Other conditions that were not controlled in this study include the age at death, storage conditions of the samples, genetic background of animals, and animal housing conditions. For these reasons, we need to be careful in interpreting the results of the analyses. It is noteworthy, however, that despite the variety of sample types used, we were able to identify some shared and distinct patterns of gene expression.

Recent attempts such as RDoC initiative have tried to reclassify psychiatric disorders according to biological domains (e.g. genes, neural circuits, behavior)[7]. While Gandal *et al* conducted non-biased coexpression analyses[8], in this study, we utilized gene groups which were derived from the findings based on the studies of animal models of neuropsychiatric disorders. Characterization by these gene groups enabled us to extract novel biological features of some neuropsychiatric disorders which are related to pseudoimmaturity inducible by neural hyperexcitation. Detecting such domains that extract the biological features of each neuropsychiatric disorder will move this diagnostic framework forward, from criteria based on signs and symptoms to those including biological dimensions.

In conclusion, biological domain, which is pseudoimmaturity inducible by neural hyperexcitation, are common endophenotype among several neuropsychiatric disorders. Future studies are needed to find translational indices that correspond to these features and can be applicable to human patients for better diagnosis of these neuropsychiatric disorders. Our findings here may promote the development of novel biomarkers, leading to better diagnosis of neuropsychiatric disorders.

(793 words)

(Main Text Total: 3967 words)

Methods

Microarray experiments to examine mouse DG development

Wild-type mouse DGs were sampled at postnatal day 8, 11, 14, 17, 21, 25, 29 (C57BL/6J × BALB/cA background; n = 5)[73], and microarray experiments were performed as previously described[10]. The microarray data, including those used in this study, were deposited in the GEO database under accession number GSE113727. We also obtained a dataset for 33-week-old wild-type mice, which we previously reported (C57BL/6J × BALB/cA background) (GSE42778)[12]. We integrated these two datasets into one to construct the dataset for the development of wild-type mouse DG used in this study (P8 versus adult, fold change > 1.2, $P < 0.05$).

Data collection and processing

Except for the mouse DG developmental dataset mentioned above, the 91 gene expression datasets used in this study were obtained from publicly available databases (listed in Table S2). All gene expression datasets were analyzed with the BaseSpace Correlation Engine (BSCE; formally known as NextBio) (https://japan.ussc.informatics.illumina.com/c/nextbio.nb; Illumina, Cupertino, CA), a database of biomedical experiments. BaseSpace is a repository of analyzed gene expression datasets that allows researchers to search expression profiles and other results[44]. The datasets registered in BaseSpace undergo several preprocessing, quality control, and organization stages. Quality control ensures the integrity of the samples and datasets and includes evaluations of pre- and postnormalization boxplots, missing value counts, and *P*-value histograms (after statistical testing) with false-discovery rate analysis to establish whether the number of significantly altered genes is larger than that expected by chance. Other microarray data processing was performed in MAS5 (Affymetrix, Santa Clara, CA, USA)[44].

Genes with a *P*-value < 0.05 (without correction for multiple testing) and an absolute fold change > 1.2 were included in the differentially expressed gene datasets. This sensitivity threshold is typically the lowest used with commercial microarray platforms and the default criterion in BaseSpace analyses[44]. All data from the Affymetrix GeneChip series were downloaded from the NCBI GEO database. Affymetrix Expression Console software (specifically the robust multiarray average algorithm) was used to preprocess the data.

We used the expression values (on a log base-2 scale) to calculate the fold changes and *P*-values between two conditions (infants–adults and patients–healthy controls). To determine the fold changes, the expression values of the probes/genes in the test data sets were

397 divided by those of the control data sets. If the fold change was < 1.0, these values were
398 converted into the negative reciprocal or −1/(fold change). Genes with an absolute fold change
399 > 1.2 and a *t*-test *P*-value < 0.05 were imported into BSCE according to the instructions
400 provided by the manufacturer. The rank order of these genes was determined by their absolute
401 fold change. We compared the signatures in two given gene sets using BSCE. All statistical
402 analyses were performed in BaseSpace and similarities between any two datasets were
403 evaluated as overlap *P*-values using the Running Fisher algorithm[44].
404 (472words)

405 **Funding and Disclosures**

406 Competing financial interests: K.T. and M.M. are employees of Astellas Pharma Inc.
407 Other authors report no biomedical financial interests.
408
409 **Acknowledgments**

410 We thank Wakako Hasegawa, Yumiko Mobayashi, Misako Murai, Tamaki
411 Murakami, Miwa Takeuchi, Yoko Kagami, Harumi Mitsuya, Aki Miyakawa and other
412 members of Miyakawa lab for their support. This work was supported by JSPS Grant-in-Aid
413 for Scientific Research on Innovative Areas Grant Number 25116526, 15H01297
414 (“Microendophenotype”), 16H06462 (“Scrap & Build”), JSPS KAKENHI Grant Number
415 25242078, and grant from Astellas Pharma Inc.
416
417 **Author Contribution Statement**

418 T.M. generated the data, performed the analysis, prepared all figures and wrote the
419 manuscript. All authors reviewed the manuscript.
420

421 **Figure legends**

422

423 ***Figure 1.***

424 The patterns of changes in gene expression in rat DG 1 day after pilocarpine
425 treatment compared with developmental changes in mouse DG and human hippocampus. Venn
426 diagrams illustrating the overlap in genome-wide gene-expression changes between rat DG
427 after seizure induction (GSE47752) and the DG of typically developing mouse infants
428 (GSE113727; P8 infants compared with 33-week adults) (a) or the hippocampus of typically
429 developing human fetuses (GSE25219: 19–23 week fetuses compared with 8–9 week fetuses)
430 (b). Bar graphs illustrate the −log of the overlap *P*-values for genes upregulated (red arrows) or
431 downregulated (green arrows) by each condition. The Bonferroni correction was used to adjust
432 the significance level according to the number of dataset pairs (see the Methods section and
433 Supplementary Method). Genes that were downregulated in both conditions were defined as
434 mouse hiM genes (green bar in (a)), and genes that were upregulated in both conditions are
435 defined as mouse hiI genes (red bar in (a)). Similarly, human hiM genes and human hiI genes
436 were defined as the groups of genes with positive correlation between the two conditions,
437 development and seizure (b).

438

439 ***Figure 2.***

440 Overview of the two-dimensional analysis (2-D analysis) for disease datasets. (a)
441 Genes with expression changes in the disease datasets are compared with the hiM and hiI gene
442 groups. The hiM- and hiI-indexes were defined as the −log of the overlap *P*-values with the
443 hiM and hiI genes. The gene expression patterns of the disease datasets are plotted in
444 two-dimensional coordinates, in which the x-/y-axes are defined by the hiM-/hiI-indexes. Each
445 dataset is characterized as hiM- or hiI- dominant by the ratio of hiM-/hiI-indexes, and the
446 degree of the hiM-/hiI-dominance are evaluated by deviation from the unity line. Distance of
447 each dataset from the origin show the degree of overlap with hiM-/hiI-genes. (b) 2-D analysis
448 applied to a dataset of postmortem brains (prefrontal cortex) from patients with schizophrenia
449 (schizophrenia dataset #1). The expression levels of 1744 genes were significantly changed in
450 this disease dataset. Of these, 87 and 76 genes overlap with the hiM/hiI genes. The overlap
451 *P*-values between the disease dataset and the hiM/hiI genes were 2.4×10^{-10} and 6.9×10^{-7}.
452 The hiM- and hiI-indexes for the disease dataset were therefore 9.62 and 6.16, indicating that
453 this dataset is hiM-dominant. The results of the 2-D analysis for this dataset are plotted in the
454 two-dimensional coordinates defined by the hiM- and hiI-indexes.

455

Figure 3.

Two-dimensional analysis (2-D analysis) for disease datasets from various neuropsychiatric disorders. Each point corresponds to the result from one independent study. (a-h) Results of the 2-D analysis of datasets for schizophrenia (a), ALS (b), Alzheimer's disease (c), autism (d), Parkinson's disease (e), bipolar disorder (f), Huntington's disease (g), and major depression (h). Filled points indicate datasets from the postmortem brain or spinal cord (ALS) of patients, and open points indicate those from cultured neural cells from patient iPSCs. (i) The distribution patterns of hiM- and hiI-index for all diseases analyzed. The extent of the changes in hiM-/hiI-indexes is assessed by the average distance of all datasets in each disease from origins. Four diseases whose average distance from origin are over 5.0 are shown as circular sectors, and others are shown as points. The radii of circular sector indicate the average distance of all datasets in each disease from origins, and the central angles of circular sector are average deviation $\pm$ sem from unity line. Each point indicates their average distance from origin and average deviation from unity line.

Figure 4.

Time-dependent changes in the hiM-/hiI-indexes in animals subjected to various putative risk events for neuropsychiatric disorders and in genetic mouse models of schizophrenia, bipolar disorder, ALS, and Alzheimer's disease. (a) Pattern of changes in the hiM- and hiI-indexes in mouse and rat hippocampus after treatment with kainite (seizure #1 (GSE1831) and seizure #2 (GSE4236)), in mouse cortex and astrocytes after middle cerebral artery occlusion (MCAO; ischemia #1 (GSE32529), ischemia #2 (GSE35338)), and in mouse cortex after CpG infection (GSE32529). (b) Pattern of changes in the hiM- and hiI-indexes of the spinal cord of an ALS mouse model with the SOD1(G93A) mutation. (c) Pattern of changes in the hiM- and hiI-indexes of the hippocampus and cortex of an Alzheimer's disease mouse model with mutations in APP and PSEN1. (d) hiM- and hiI-indexes in mouse models of schizophrenia and bipolar disorder.

Table 1.

Summary of results from the pathway analyses of hiM/hiI genes. (a) The 20 biogroups with the most significant similarities to mouse hiM genes and mouse hiI genes. Green columns indicate biogroups that are related to the plasma membrane. Red columns indicate biogroups that are related to reactions in the nucleus. (b) The 20 biogroups with the most significant similarities to human hiM genes and human hiI genes.

(790 words, 4 figures, 1 table)

491

References

1. Cross-national comparisons of the prevalences and correlates of mental disorders. WHO International Consortium in Psychiatric Epidemiology. *Bull World Health Organ* **78,** 413–426 (2000).

2. Cardno, A. G. & Owen, M. J. Genetic Relationships Between Schizophrenia, Bipolar Disorder, and Schizoaffective Disorder. *Schizophr Bull* **40,** 504–515 (2014).

3. Hall, J., Trent, S., Thomas, K. L., O'Donovan, M. C. & Owen, M. J. Genetic Risk for Schizophrenia: Convergence on Synaptic Pathways Involved in Plasticity. *Biological Psychiatry* **77,** 52–58 (2015).

4. Forero, D. A. *et al.* A network of synaptic genes associated with schizophrenia and bipolar disorder. *Schizophrenia Research* **172,** 68–74 (2016).

5. Douaud, G. *et al.* A common brain network links development, aging, and vulnerability to disease. *PNAS* **111,** 17648–17653 (2014).

6. Argyelan, M. *et al.* Resting-State fMRI Connectivity Impairment in Schizophrenia and Bipolar Disorder. *Schizophr Bull* **40,** 100–110 (2014).

7. Insel, T. R. & Cuthbert, B. N. Brain disorders? Precisely. *Science* **348,** 499–500 (2015).

8. Gandal, M. J. *et al.* Shared molecular neuropathology across major psychiatric disorders parallels polygenic overlap. *Science* **359,** 693–697 (2018).

9. Hagihara, H., Takao, K., Walton, N. M., Matsumoto, M. & Miyakawa, T. Immature Dentate Gyrus: An Endophenotype of Neuropsychiatric Disorders. *Neural Plasticity* **2013,** (2013).

10. Yamasaki, N. *et al.* Alpha-CaMKII deficiency causes immature dentate gyrus, a novel candidate endophenotype of psychiatric disorders. *Molecular Brain* **1,** 6 (2008).

11. Ohira, K. *et al.* Synaptosomal-associated protein 25 mutation induces immaturity of the dentate granule cells of adult mice. *Molecular Brain* **6,** 12 (2013).

12. Takao, K. *et al.* Deficiency of Schnurri-2, an MHC Enhancer Binding Protein, Induces Mild Chronic Inflammation in the Brain and Confers Molecular, Neuronal, and Behavioral Phenotypes Related to Schizophrenia. *Neuropsychopharmacology* **38,** 1409–1425 (2013).

13. Hagihara, H. *et al.* Circadian Gene Circuitry Predicts Hyperactive Behavior in a Mood Disorder Mouse Model. *Cell Reports* **14,** 2784–2796 (2016).

14. Nakao, A. *et al.* Immature morphological properties in subcellular-scale structures in the dentate gyrus of Schnurri-2 knockout mice: a model for schizophrenia and

527 intellectual disability. *Molecular Brain* **10,** 60 (2017).
528 15. Hagihara, H., Fujita, M., Umemori, J., Hashimoto, M. & Miyakawa, T.
529 Immature-like molecular expression patterns in the hippocampus of a mouse model of
530 dementia with Lewy body-linked mutant β-synuclein. (2018).
531 16. Shin, R. *et al.* The immature dentate gyrus represents a shared phenotype
532 of mouse models of epilepsy and psychiatric disease. *Bipolar Disord* **15,** 405–421 (2013).
533 17. You, J. C. *et al.* Epigenetic suppression of hippocampal calbindin-D28k by
534 ΔFosB drives seizure-related cognitive deficits. *Nature Medicine* **23,** 1377 (2017).
535 18. Maglóczky, Z., Halász, P., Vajda, J., Czirják, S. & Freund, T. F. Loss of
536 Calbindin-D28K immunoreactivity from dentate granule cells in human temporal lobe
537 epilepsy. *Neuroscience* **76,** 377–385 (1997).
538 19. Karádi, K. *et al.* Correlation between calbindin expression in granule cells
539 of the resected hippocampal dentate gyrus and verbal memory in temporal lobe epilepsy.
540 *Epilepsy & Behavior* **25,** 110–119 (2012).
541 20. Zhang, Z. J. & Reynolds, G. P. A selective decrease in the relative density
542 of parvalbumin-immunoreactive neurons in the hippocampus in schizophrenia. *Schizophrenia*
543 *Research* **55,** 1–10 (2002).
544 21. Hashimoto, T. *et al.* Gene Expression Deficits in a Subclass of GABA
545 Neurons in the Prefrontal Cortex of Subjects with Schizophrenia. *J. Neurosci.* **23,** 6315–6326
546 (2003).
547 22. Fung, S. J. *et al.* Expression of Interneuron Markers in the Dorsolateral
548 Prefrontal Cortex of the Developing Human and in Schizophrenia. *AJP* **167,** 1479–1488
549 (2010).
550 23. Pantazopoulos, H., Woo, T.-U. W., Lim, M. P., Lange, N. & Berretta, S.
551 Extracellular Matrix-Glial Abnormalities in the Amygdala and Entorhinal Cortex of Subjects
552 Diagnosed With Schizophrenia. *Arch Gen Psychiatry* **67,** 155–166 (2010).
553 24. Berretta, S. Extracellular matrix abnormalities in schizophrenia.
554 *Neuropharmacology* **62,** 1584–1597 (2012).
555 25. Hagihara, H., Ohira, K., Takao, K. & Miyakawa, T. Transcriptomic
556 evidence for immaturity of the prefrontal cortex in patients with schizophrenia. *Molecular*
557 *Brain* **7,** 41 (2014).
558 26. Gandal, M. J., Nesbitt, A. M., McCurdy, R. M. & Alter, M. D. Measuring
559 the Maturity of the Fast-Spiking Interneuron Transcriptional Program in Autism,
560 Schizophrenia, and Bipolar Disorder. *PLOS ONE* **7,** e41215 (2012).
561 27. Mellios, N. *et al.* Molecular Determinants of Dysregulated GABAergic

562 Gene Expression in the Prefrontal Cortex of Subjects with Schizophrenia. *Biological*
563 *Psychiatry* **65,** 1006–1014 (2009).
564 28. Hashimoto, T. *et al.* Alterations in GABA-related transcriptome in the
565 dorsolateral prefrontal cortex of subjects with schizophrenia. *Mol. Psychiatry* **13,** 147–161
566 (2008).
567 29. Murano, T., Koshimizu, H., Hagihara, H. & Miyakawa, T. Transcriptomic
568 immaturity of the hippocampus and prefrontal cortex in patients with alcoholism. *Scientific*
569 *Reports* **7,** srep44531 (2017).
570 30. Kobayashi, K. *et al.* Reversal of hippocampal neuronal maturation by
571 serotonergic antidepressants. *Proceedings of the National Academy of Sciences* **107,**
572 8434–8439 (2010).
573 31. Ohira, K., Takeuchi, R., Iwanaga, T. & Miyakawa, T. Chronic fluoxetine
574 treatment reduces parvalbumin expression and perineuronal netsin gamma-aminobutyric
575 acidergic interneurons of the frontal cortex in adultmice. *Molecular Brain* **6,** 43 (2013).
576 32. Imoto, Y., Segi-Nishida, E., Suzuki, H. & Kobayashi, K. Rapid and stable
577 changes in maturation-related phenotypes of the adult hippocampal neurons by
578 electroconvulsive treatment. *Molecular Brain* **10,** 8 (2017).
579 33. Chang, Y.-T. *et al.* Bidirectional relation between schizophrenia and
580 epilepsy: A population-based retrospective cohort study. *Epilepsia* **52,** 2036–2042 (2011).
581 34. Hyde, T. M. & Weinberger, D. R. Seizures and schizophrenia. *Schizophr*
582 *Bull* **23,** 611–622 (1997).
583 35. Cascella, N. G., Schretlen, D. J. & Sawa, A. SCHIZOPHRENIA AND
584 EPILEPSY: IS THERE A SHARED SUSCEPTIBILITY? *Neuroscience research* **63,** 227
585 (2009).
586 36. Coyle, J. T. Glutamate and Schizophrenia: Beyond the Dopamine
587 Hypothesis. *Cell Mol Neurobiol* **26,** 363–382 (2006).
588 37. Mouri, A., Noda, Y., Enomoto, T. & Nabeshima, T. Phencyclidine animal
589 models of schizophrenia: Approaches from abnormality of glutamatergic neurotransmission
590 and neurodevelopment. *Neurochemistry International* **51,** 173–184 (2007).
591 38. Kehrer, C., Maziashvili, N., Dugladze, T. & Gloveli, T. Altered
592 Excitatory-Inhibitory Balance in the NMDA-Hypofunction Model of Schizophrenia. *Front*
593 *Mol Neurosci* **1,** (2008).
594 39. O'Donnell, C., Gonçalves, J. T., Portera-Cailliau, C. & Sejnowski, T. J.
595 Beyond excitation/inhibition imbalance in multidimensional models of neural circuit changes
596 in brain disorders. *eLife* **6,**

40. Mertens, J. *et al.* Differential responses to lithium in hyperexcitable neurons from patients with bipolar disorder. *Nature* **527,** 95–99 (2015).

41. Vossel, K. A. *et al.* Incidence and impact of subclinical epileptiform activity in Alzheimer's disease. *Annals of Neurology* **80,** 858–870

42. Lam, A. D. *et al.* Silent Hippocampal Seizures and Spikes Identified by Foramen Ovale Electrodes in Alzheimer's Disease. *Nat Med* **23,** 678–680 (2017).

43. Vossel, K. A., Tartaglia, M. C., Nygaard, H. B., Zeman, A. Z. & Miller, B. L. Epileptic activity in Alzheimer's disease: causes and clinical relevance. *The Lancet Neurology* **16,** 311–322 (2017).

44. Kupershmidt, I. *et al.* Ontology-Based Meta-Analysis of Global Collections of High-Throughput Public Data. *PLOS ONE* **5,** e13066 (2010).

45. Takao, K. & Miyakawa, T. Genomic responses in mouse models greatly mimic human inflammatory diseases. *PNAS* **112,** 1167–1172 (2015).

46. Ryan, S. D. *et al.* Isogenic Human iPSC Parkinson's Model Shows Nitrosative Stress-Induced Dysfunction in MEF2-PGC1α Transcription. *Cell* **155,** 1351–1364 (2013).

47. Dingledine, R. *et al.* Data Descriptor: Transcriptional profile of hippocampal dentate granule cells in four rat epilepsy models. *Scientific Data* **4,** (2017).

48. Kang, H. J. *et al.* Spatio-temporal transcriptome of the human brain. *Nature* **478,** 483–489 (2011).

49. van Os, J., Kenis, G. & Rutten, B. P. F. The environment and schizophrenia. *Nature* **468,** 203–212 (2010).

50. DeMichele-Sweet, M. a. A. *et al.* Genetic risk for schizophrenia and psychosis in Alzheimer disease. *Molecular Psychiatry* (2017). doi:10.1038/mp.2017.81

51. Wilson, D. N. *et al.* Microarray analysis of postictal transcriptional regulation of neuropeptides. *J Mol Neurosci* **25,** 285 (2005).

52. Hermey, G. *et al.* Genome-Wide Profiling of the Activity-Dependent Hippocampal Transcriptome. *PLOS ONE* **8,** e76903 (2013).

53. Vartanian, K. B. *et al.* LPS preconditioning redirects TLR signaling following stroke: TRIF-IRF3 plays a seminal role in mediating tolerance to ischemic injury. *Journal of Neuroinflammation* **8,** 140 (2011).

54. Stevens, S. L. *et al.* Multiple Preconditioning Paradigms Converge on Interferon Regulatory Factor-Dependent Signaling to Promote Tolerance to Ischemic Brain Injury. *J. Neurosci.* **31,** 8456–8463 (2011).

55. Nardo, G. *et al.* Transcriptomic indices of fast and slow disease

632 progression in two mouse models of amyotrophic lateral sclerosis. *Brain* **136,** 3305–3332
633 (2013).
634 56. Lerman, B. J. *et al.* Deletion of galectin-3 exacerbates microglial
635 activation and accelerates disease progression and demise in a SOD1 G93A mouse model of
636 amyotrophic lateral sclerosis. *Brain and Behavior* **2,** 563–575 (2012).
637 57. Matarin, M. *et al.* A Genome-wide Gene-Expression Analysis and
638 Database in Transgenic Mice during Development of Amyloid or Tau Pathology. *Cell Reports*
639 **10,** 633–644 (2015).
640 58. Xu, B., Hsu, P.-K., Stark, K. L., Karayiorgou, M. & Gogos, J. A.
641 Derepression of a Neuronal Inhibitor due to miRNA Dysregulation in a Schizophrenia-Related
642 Microdeletion. *Cell* **152,** 262–275 (2013).
643 59. Srivastava, S. *et al.* Loss-of-function variants in *HIVEP2* are a cause of
644 intellectual disability. *European Journal of Human Genetics* **24,** 556–561 (2016).
645 60. Steinfeld, H. *et al.* Mutations in HIVEP2 are associated with
646 developmental delay, intellectual disability, and dysmorphic features. *Neurogenetics* **17,**
647 159–164 (2016).
648 61. Harrison, P. J. The hippocampus in schizophrenia: a review of the
649 neuropathological evidence and its pathophysiological implications. *Psychopharmacology* **174,**
650 151–162 (2004).
651 62. Glausier, J. R. & Lewis, D. A. Dendritic spine pathology in schizophrenia.
652 *Neuroscience* **251,** 90–107 (2013).
653 63. Fatemi, S. H., Folsom, T. D. & Thuras, P. D. GABAA and GABAB
654 receptor dysregulation in superior frontal cortex of subjects with schizophrenia and bipolar
655 disorder. *Synapse* **71,** (2017).
656 64. Lisman, J. E. *et al.* Circuit-based framework for understanding
657 neurotransmitter and risk gene interactions in schizophrenia. *Trends Neurosci.* **31,** 234–242
658 (2008).
659 65. Chestnut, B. A. *et al.* Epigenetic Regulation of Motor Neuron Cell Death
660 through DNA Methylation. *J. Neurosci.* **31,** 16619–16636 (2011).
661 66. Martin, L. J. & Wong, M. Aberrant Regulation of DNA Methylation in
662 Amyotrophic Lateral Sclerosis: A New Target of Disease Mechanisms. *Neurotherapeutics* **10,**
663 722–733 (2013).
664 67. Nguyen, M. D. *et al.* Cell Cycle Regulators in the Neuronal Death Pathway
665 of Amyotrophic Lateral Sclerosis Caused by Mutant Superoxide Dismutase 1. *J. Neurosci.* **23,**
666 2131–2140 (2003).

68. Dorszewska, J. *et al.* Mutations of TP53 Gene and Oxidative Stress in Alzheimer's Disease Patients. *Advances in Alzheimer's Disease* **03,** 24 (2014).

69. Moskalev, A. A. *et al.* Gadd45 proteins: Relevance to aging, longevity and age-related pathologies. *Ageing Research Reviews* **11,** 51–66 (2012).

70. Brennand, K. J. *et al.* Modelling schizophrenia using human induced pluripotent stem cells. *Nature* **473,** 221–225 (2011).

71. Wen, Z. *et al.* Synaptic dysregulation in a human iPS cell model of mental disorders. *Nature* **515,** 414–418 (2014).

72. Chan, M. K. *et al.* Evidence for disease and antipsychotic medication effects in post-mortem brain from schizophrenia patients. *Mol Psychiatry* **16,** 1189–1202 (2011).

73. Hagihara, H., Toyama, K., Yamasaki, N. & Miyakawa, T. Dissection of hippocampal dentate gyrus from adult mouse. *J Vis Exp* (2009). doi:10.3791/1543

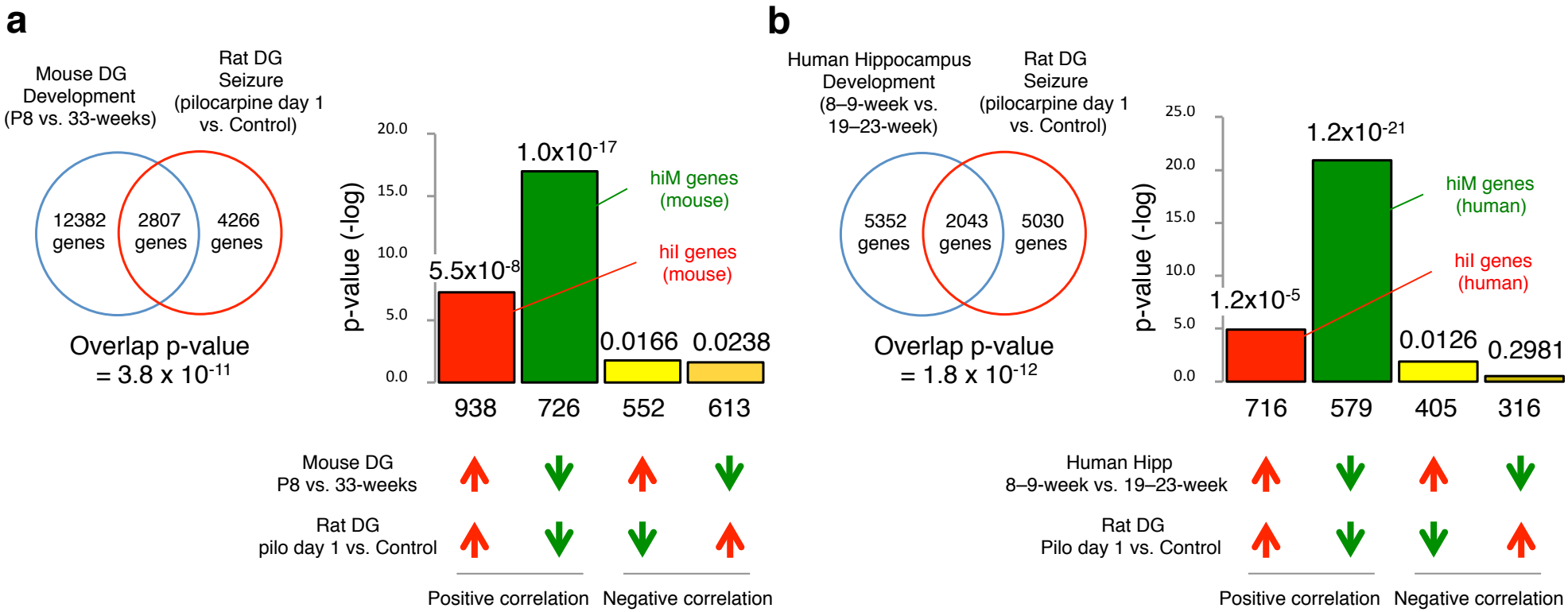
a
Mouse DG
Development
(P8 vs. 33-weeks)
Rat DG
Seizure
(pilocarpine day 1
vs. Control)
12382
genes
2807
genes
4266
genes
Overlap p-value
= 3.8 x 10-11
p-value (-log)
20.0
15.0
10.0
5.0
0.0
5.5x10-8
1.0x10-17
0.0166
0.0238
hiM genes
(mouse)
hiI genes
(mouse)
938
726
552
613
Mouse DG
P8 vs. 33-weeks
Rat DG
pilo day 1 vs. Control
Positive correlation
Negative correlation
b
Human Hippocampus
Development
(8–9-week vs.
19–23-week)
Rat DG
Seizure
(pilocarpine day 1
vs. Control)
5352
genes
2043
genes
5030
genes
Overlap p-value
= 1.8 x 10-12
p-value (-log)
25.0
20.0
15.0
10.0
5.0
0.0
1.2x10-5
1.2x10-21
0.0126
0.2981
hiM genes
(human)
hiI genes
(human)
716
579
405
316
Human Hipp
8–9-week vs. 19–23-week
Rat DG
Pilo day 1 vs. Control
Positive correlation
Negative correlation

Figure 1

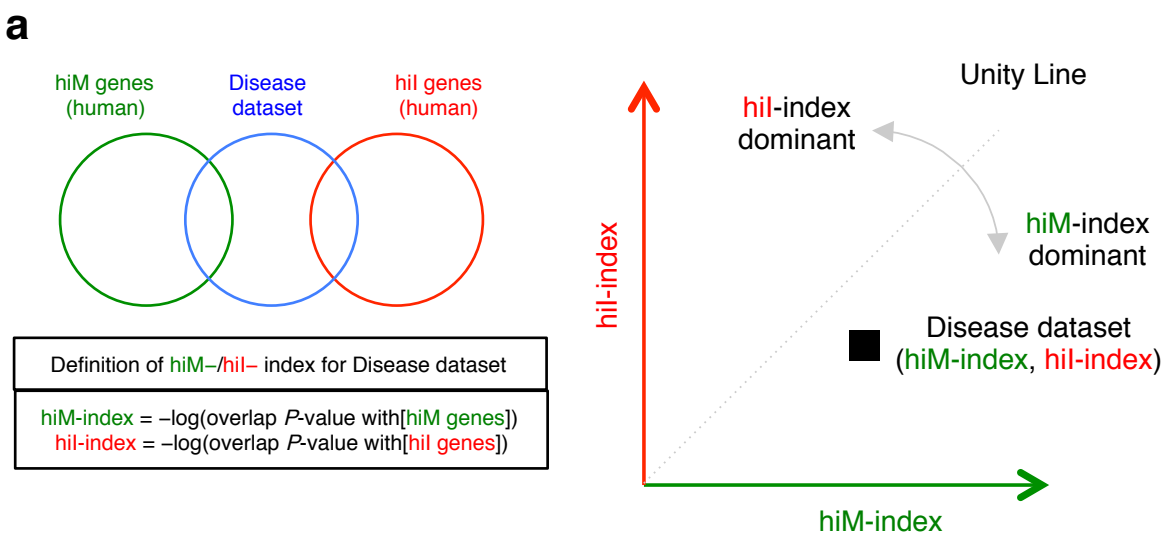
a
hiM genes (human)
Disease dataset
hiI genes (human)
Definition of hiM–/hiI– index for Disease dataset
hiM-index = –log(overlap P-value with[hiM genes])
hiI-index = –log(overlap P-value with[hiI genes])
Unity Line
hiI-index dominant
hiM-index dominant
Disease dataset (hiM-index, hiI-index)
hiI-index
hiM-index

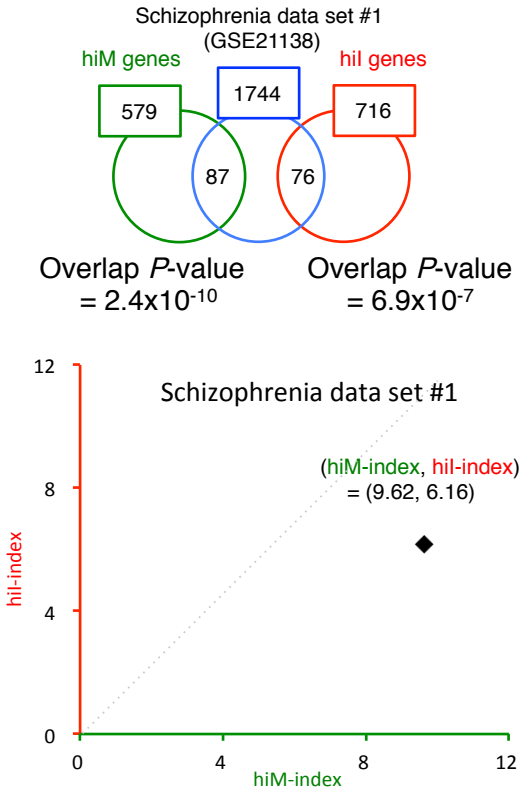
b
Schizophrenia data set #1 (GSE21138)
hiM genes
hiI genes
579
1744
716
87
76
Overlap P-value = 2.4x10-10
Overlap P-value = 6.9x10-7
Schizophrenia data set #1
(hiM-index, hiI-index) = (9.62, 6.16)
hiI-index
hiM-index
0
4
8
12

Figure 2

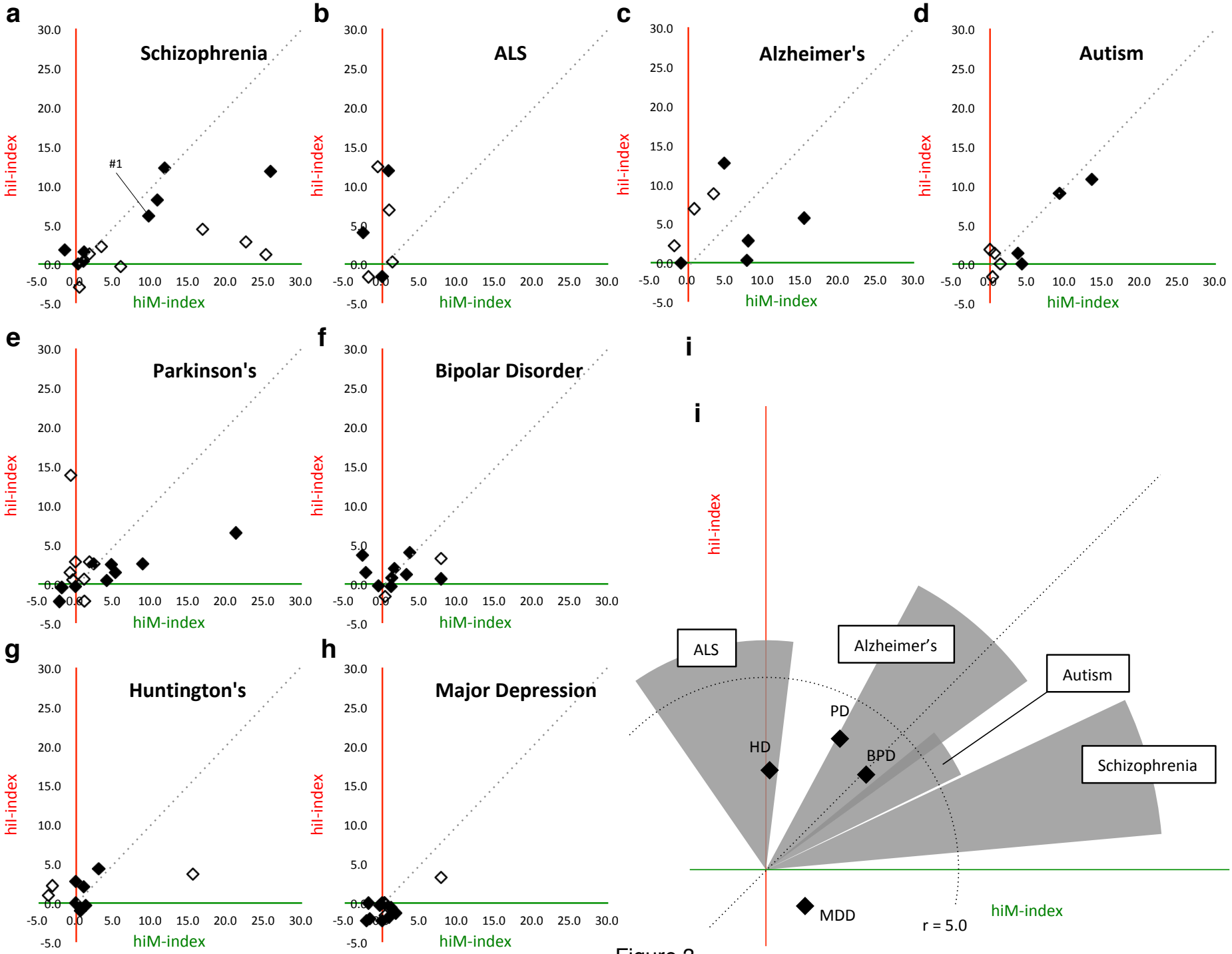
a
Schizophrenia
#1
b
ALS
c
Alzheimer's
d
Autism
e
Parkinson's
f
Bipolar Disorder
g
Huntington's
h
Major Depression
hil-index
hiM-index
i
ALS
Alzheimer's
Autism
Schizophrenia
PD
HD
BPD
MDD
r = 5.0

Figure 3

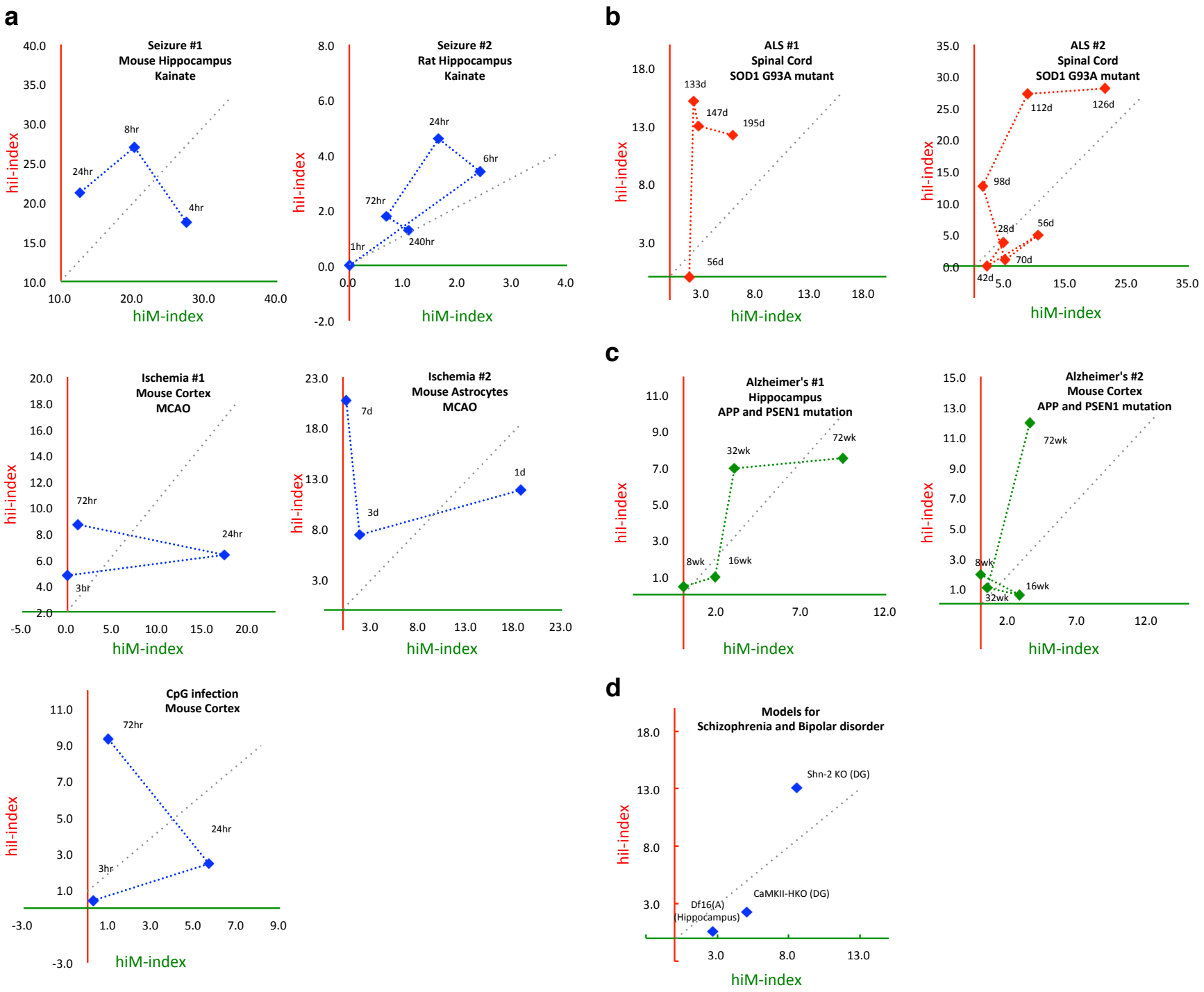
a
Seizure #1
Mouse Hippocampus
Kainate
24hr
8hr
4hr
Seizure #2
Rat Hippocampus
Kainate
24hr
6hr
72hr
1hr
240hr
b
ALS #1
Spinal Cord
SOD1 G93A mutant
133d
147d
195d
56d
ALS #2
Spinal Cord
SOD1 G93A mutant
112d
126d
98d
28d
56d
70d
42d
c
Ischemia #1
Mouse Cortex
MCAO
72hr
24hr
3hr
Ischemia #2
Mouse Astrocytes
MCAO
7d
3d
1d
Alzheimer's #1
Hippocampus
APP and PSEN1 mutation
72wk
32wk
8wk
16wk
Alzheimer's #2
Mouse Cortex
APP and PSEN1 mutation
72wk
8wk
16wk
32wk
CpG infection
Mouse Cortex
72hr
24hr
3hr
d
Models for
Schizophrenia and Bipolar disorder
Shn-2 KO (DG)
CaMKII-HKO (DG)
Df16(A)
(Hippocampus)
hil-index
hiM-index

Figure 4

a

Table 1

hiM genes (mouse)			
Biogroup name	direction	Common genes	p-value
multicellular organismal signaling	down	56	4.00E-23
transmission of nerve impulse	down	51	3.10E-19
axon	down	45	7.30E-19
neuron differentiation	down	58	4.70E-17
synapse	down	57	5.70E-17
neuron development	down	50	1.50E-16
neuronal cell body	down	45	5.20E-16
cell junction	down	56	3.00E-15
cell part morphogenesis	down	43	4.70E-15
neuron projection development	down	42	6.20E-15
cell projection part	down	56	6.50E-15
cell morphogenesis involved in neuron differentiation	down	35	2.90E-14
cell morphogenesis involved in differentiation	down	40	6.70E-14
cellular chemical homeostasis	down	53	2.50E-13
cell-cell signaling	down	44	2.60E-13
synaptic transmission	down	37	3.60E-13
regulation of neurological system process	down	31	1.10E-12
regulation of transmission of nerve impulse	down	30	1.40E-12
Genes involved in Neuronal System	down	31	1.70E-12
cellular ion homeostasis	down	49	1.80E-12

hiI genes (mouse)			
Biogroup name	direction	Common genes	p-value
response to wounding	up	60	1.10E-16
positive regulation of developmental process	up	66	9.30E-16
cardiovascular system development	up	61	7.70E-15
circulatory system development	up	61	7.70E-15
proteinaceous extracellular matrix	up	32	7.80E-15
Genes involved in Cell Cycle	up	47	1.00E-14
extracellular matrix	up	37	1.30E-14
Genes involved in Cell Cycle, Mitotic	up	42	6.30E-14
protein domain specific binding	up	60	7.00E-14
positive regulation of signal transduction	up	58	8.70E-14
Genes involved in DNA Replication	up	32	9.20E-14
cell cycle	up	67	3.00E-13
Genes involved in Adaptive Immune System	up	56	3.20E-13
Focal adhesion	up	31	5.60E-13
kinase binding	up	44	5.50E-12
cytoskeleton organization	up	54	5.60E-12
neuron differentiation	up	52	5.80E-12
basement membrane	up	19	7.50E-12
regulation of cell migration	up	36	1.10E-11
MAPKinase Signaling Pathway	up	20	1.40E-11

b

hiM genes (human)			
Biogroup name	direction	Common genes	p-value
multicellular organismal signaling	up	87	4.40E-58
transmission of nerve impulse	up	83	1.40E-54
synaptic transmission	up	75	6.70E-50
neuron projection	up	70	2.60E-44
axon	up	42	2.90E-33
synapse	up	51	2.60E-32
neuron development	up	58	1.60E-30
Genes involved in Neuronal System	up	41	3.40E-30
Genes involved in Transmission across Chemical Synapses	up	32	1.50E-29
regulation of neurological system process	up	35	6.50E-29
regulation of transmission of nerve impulse	up	34	9.20E-29
cell projection part	up	53	1.80E-27
passive transmembrane transporter activity	up	44	1.80E-26
ion channel activity	up	43	2.20E-26
cell part morphogenesis	up	49	1.80E-24
behavior	up	38	2.90E-24
single-organism behavior	up	35	3.70E-24
cell morphogenesis involved in neuron differentiation	up	44	4.30E-24
neuron projection development	up	47	4.40E-24
dendrite	up	37	2.00E-23

hiI genes (human)			
Biogroup name	direction	Common genes	p-value
chromosome	down	65	1.30E-32
response to DNA damage stimulus	down	60	4.80E-32
Genes involved in Cell Cycle	down	50	3.60E-31
Genes involved in Cell Cycle, Mitotic	down	43	1.20E-30
Genes involved in DNA Replication	down	34	2.00E-30
interphase	down	47	8.20E-30
interphase of mitotic cell cycle	down	46	5.10E-29
Genes involved in Mitotic M-M/G1 phases	down	29	2.60E-26
Cell cycle	down	25	7.60E-23
DNA repair	down	40	2.30E-22
wound healing	down	50	7.40E-22
response to ionizing radiation	down	21	1.20E-20
nuclear division	down	35	8.00E-20
mitosis	down	35	8.00E-20
cell division	down	38	2.20E-19
G1/S transition of mitotic cell cycle	down	26	1.70E-18
cardiovascular system development	down	46	3.20E-18
circulatory system development	down	46	3.20E-18
S phase	down	22	3.80E-18
blood coagulation	down	41	6.10E-18